Contribution from the Department of Chemistry, West Virginia University, Morgantown, West Virginia 26506, the Chemistry Division, Argonne National Laboratory, Argonne, Illinois 60439, and the Department of Chemistry, Brookhaven National Laboratory, Upton, New York 11973

Single-Crystal Neutron Diffraction Study (17 K) of the Unusual Cr–D–Cr Bond in $[(Ph_3P)_2N]^+[Cr_2(CO)_{10}(\mu\text{-}D)]^-$. Evidence for a Four-Site Distribution of the Bridging Deuterium Atom[1]

JEFFREY L. PETERSEN,*[2a] RICHARD K. BROWN,[2b,c] JACK M. WILLIAMS,*[2b] and RICHARD K. McMULLAN[2d]

Received April 17, 1979

A low-temperature (17 ± 2 K) neutron diffraction study of $[(Ph_3P)_2N]^+[Cr_2(CO)_{10}(\mu\text{-}D)]^-$ (ca. 85% deuterated) has been carried out to examine the nature of the Cr–D–Cr bond in the monoanion. The nondeuterium atoms are located with high precision and there is no indication of a metal carbonyl structural disorder. Only one peak is resolved for the bridging D atom, at the midpoint of the Cr–Cr line located on a crystallographic center of symmetry. The D atom's root-mean-square thermal displacements (obtained from an anisotropic refinement) are several times larger than those for the remaining atoms and reflect a disordered structure for the D atom within the plane normal to the Cr–Cr line. Assuming equal population of four off-axis disordered D sites (which are staggered with respect to the four Cr–CO(eq) directions), a least-squares refinement (based on F_o^2) demonstrates that the data accommodate this disordered model. Due to the close proximity of these disordered sites and the relatively large zero-point energy of the μ-D atom, the averaging nature of the diffraction experiment provides only a composite picture of the disordered structure in this case. Consequently, our interpretation is limited by the inherent limitations associated with diffraction methods and points out the need for further solid-state spectroscopic studies to obtain more detailed information about the nature of this unusual disorder. The neutron-determined lattice parameters for the monoclinic cell, $C2/c$, are a = 21.148 (7) Å, b = 16.004 (7) Å, c = 15.819 (8) Å, and β = 127.77 (4)° for λ 1.1602 (1) Å. The agreements obtained for the two refinement models of the μ-D atom (i.e., ordered/anisotropic and disordered/isotropic) are identical. The final discrepancy indices for the fourfold disordered model are $R(F_o)$ = 0.0377, $R(F_o^2)$ = 0.0398, $R_w(F_o^2)$ = 0.0518, and σ_1 = 1.21 for 4191 reflections with $F_o^2 > \sigma(F_o^2)$. The corresponding Cr–D–Cr bond angles and Cr–D bond distances agree with those determined from an earlier room-temperature study of $[Et_4N]^+$-$[Cr_2(CO)_{10}(\mu\text{-}H)]^-$, in which the twofold disordered structure for the bridging atom was resolved.

Introduction

Binuclear metal carbonyl hydrides of the type $[M_2(CO)_{10}(\mu\text{-}H)]^-$ (M = Cr, Mo, W) have attracted considerable interest because of their unusual molecular structures[3,4] and chemical reactivity.[5] Our neutron diffraction studies of the $[Et_4N]^+$ [3a] and $[(Ph_3P)_2N]^+$ [3b] salts of the $[Cr_2(CO)_{10}(\mu\text{-}H)]^-$ monoanion have revealed unexpectedly that the bridging H atom is displaced ca. 0.3 Å from the midpoint of the Cr–Cr line in an apparently "closed-type"[6] Cr–H–Cr bond. A twofold off-axis disorder of the bridging H atom was resolved at room temperature for the $[Et_4N]^+$ salt, while only one bridging H atom position (at the center of symmetry) was observed for the $[(Ph_3P)_2N]^+$ salt. However, in the latter salt, the unusual H atom thermal ellipsoid suggests that the observed structural parameters represent a composite of at least a fourfold disorder of this atom. Although the nature of the bridging H atom structure in the two salts differs, the nonhydrogen backbone of the anion does not deviate substantially from a pseudo-D_{4h} geometry.

To determine the level of the disorder and to provide a basis for comparison with our room-temperature results,[3b] we have undertaken a low-temperature (17 K) single-crystal neutron diffraction study of $[(Ph_3P)_2N]^+[Cr_2(CO)_{10}(\mu\text{-}D)]^-$. The deuterium analogue was chosen because of its more favorable scattering length (viz.: D, 0.672×10^{-12} cm; H, -0.372×10^{-12} cm) and larger mass which collectively should improve the observability of the bridging atom's position.

Experimental Section

Crystal Preparation. Suitable crystals (10–20 mg) of $[(Ph_3P)_2N]^+[Cr_2(CO)_{10}(\mu\text{-}D)]^-$ were grown from saturated and degassed ethanol solutions by slow evaporation. The solutions were placed in a desiccator over $Mg(ClO_4)_2$ and then cooled in a refrigerator to initiate crystallization. Deuterated samples were prepared by published methods[7,8] with $NaBD_4$ as the reducing agent and were kindly supplied by T. Hall of Dr. J. K. Ruff's research group (University of Georgia).

Collection and Structural Analysis of Neutron Diffraction Data. A 12-mg single crystal of $[(Ph_3P)_2N]^+[Cr_2(CO)_{10}(\mu\text{-}D)]^-$, with approximate dimensions of 0.90 × 1.85 × 5.80 mm, was mounted on an aluminum pin in a helium-filled chamber of a Displex cryogenic refrigerator. A total of 4817 three-dimensional data were collected on the Chemistry Division four-circle neutron diffractometer at the Brookhaven high-flux beam reactor. All data (hkl and $hk\bar{l}$) were collected at 17 ± 2 K out to $(\sin\theta)/\lambda$ = 0.684 Å^{-1} (λ 1.1602 (1) Å, based on KBr, a = 6.6000 Å; Ge(220) monochromator). A least-squares fit of 32 automatically centered reflections (48° ≤ 2θ ≤ 64°) confirmed the monoclinic unit cell ($C2/c$) (C_{2h}^6, No. 15) with a = 21.148 (7) Å, b = 16.004 (7) Å, c = 15.819 (8) Å, β = 127.77 (4)°, V_c = 4232.2 Å^3, and d_{calcd} = 1.452 g cm^{-3} for Z = 4. Data were collected by the usual ω–2θ step-scan procedure. For reflections with 2θ ≤ 50°, a preset scan width of 3.44°(2θ), consisting of 86 steps of 0.04° each, was used. For reflections with 2θ > 50° the scan width $\Delta(2\theta)$ was determined from the formula

$$\Delta(2\theta) = A + B \tan\theta$$

where A and B were determined from an experimental dispersion curve to be 1.30 and 4.16, respectively. In this region the step size (0.04–0.09°) and number of steps (66–96) were varied. Reference reflections were measured every 50 reflections and a maximum fluctuation of only 4% was observed. Background counts were estimated from 10% of the scan at each peak extremity. Integrated intensities (I) were calculated from

$$I = \left[P - \frac{n_P}{n_B}(B_1 + B_2) \right] SN$$

and $\sigma_c(I)$ was calculated from counting statistics by

$$\sigma_c(I) = \left[P + \left(\frac{n_P}{n_B}\right)^2 (B_1 + B_2) \right]^{1/2} SN$$

where P is the total peak count, B_1 and B_2 are the background counts, SN is a normalization factor to account for step size and monitor count, and n_P and n_B are the number of steps for the peak and background, respectively. Integrated intensities were corrected for Lorentz and absorption (μ_c = 1.31 cm^{-1}) effects and the range of transmission coefficients was 0.723–0.839. Duplicate reflections were averaged, yielding 4691 independent reflections (4191 had $F_o^2 \geq \sigma(F_o^2)$).

The least-squares refinement was initiated by using the positional parameters obtained from our room-temperature neutron diffraction study[3b] of $[(Ph_3P)_2N]^+[Cr_2(CO)_{10}(\mu\text{-}H)]^-$ and with isotropic temperature factors set at B = 1.5 Å^2. Two cycles of least-squares refinement on F_o^2 for all atoms except the bridging D atom led to discrepancy indices[9] of $R(F_o)$ = 0.086, $R(F_o^2)$ = 0.100, and $R_w(F_o^2)$

0020-1669/79/1318-3493$01.00/0

Table I. Final Discrepancy Indices

refinement	one μ-D site anisotropic model		four μ-D site disordered model	
	all data	$F_o^2 > \sigma(F_o^2)$	all data	$F_o^2 > \sigma(F_o^2)$
no. of reflections	4691	4191	4691	4191
$R(F_o)$	0.0473	0.0374	0.0475	0.0377
$R(F_o^2)$	0.0416	0.0396	0.0418	0.0398
$R_w(F_o^2)$	0.0647	0.0519	0.0646	0.0518
σ_1[a]	1.43	1.22	1.42	1.21
S[b]	0.889 (1)		0.889 (1)	
g	0.129 (13) × 10^{-4}		0.126 (13) × 10^{-4}	

[a] σ_1, the standard deviation of an observation of unit weight, is defined by $[\Sigma w_i|F_o^2 - F_c^2|/(n-p)]^{1/2}$ with $w_i^{-1} = \sigma^2(F_o^2) = \sigma_c^2(F_o^2) + (0.02F_o^2)^2$, where $\sigma_c(F_o^2)$ is determined by counting statistics, n is the number of observations, and p is the number of parameters varied (viz., 418 (anisotropic) or 419 (fourfold disorder)) during the least-squares refinement. Including all of the data, the data-to-parameter ratio is 11.2:1. [b] Scale factor.

= 0.100. A difference Fourier map then revealed only one large positive peak at $x = 0.0$, $y = 0.0$, and $z = 0.0$. To our surprise the inclusion of the D atom in the refinement led to a very large isotropic temperature factor of $B = 9.0$ Å^2 while those for the remaining atoms of the monoanion ranged from only 0.3 to 1.0 Å^2. This suggested either unusually high anisotropic thermal motion for the D atom or a disordered structure. Several cycles of full-matrix least-squares refinement of the positional and anisotropic thermal factors for the monoanion atoms clearly revealed that the largest D atom thermal displacements are directed normal to the Cr–Cr axis. Careful examination of the agreement between F_o and F_c indicated a small systematic variation due to extinction, and an isotropic secondary extinction parameter g[10-12] was introduced. After two cycles of full-matrix refinement the percent deuteration was estimated by fixing the atomic parameters and then varying the scattering lengths of all the atoms. The D atom scattering length decreased from 0.672 × 10^{-12} to 0.520 × 10^{-12} cm, indicating that the anion is more than 85% deuterated. The remaining scattering lengths did not vary by more than 0.5% from their assigned values.[13,14] Since the sample is not completely deuterated, the anion's structure will contain contributions from both H and D. Because the two isotopes provide different zero-point energies for the Cr–(H/D)–Cr vibrational modes, the data should reflect a weighted average of their individual contributions. Although this problem is unlikely to modify appreciably our overall interpretation, it probably will smear out the subtle structural details which may accompany a disordered structure (vide infra). With an experimentally determined scattering length for the bridging D atom in the anion, two additional cycles of anisotropic full-matrix least-squares refinement led to the final discrepancy indices given in Table I. At the conclusion of the refinement, the final change-to-esd ratio was less than 0.1 for most parameters.

Since the magnitude of the bridging atom's thermal ellipsoid is not reduced significantly with temperature, one must conclude that the observed thermal motion is due to the spatial averaging of several disordered sites rather than the vibrational motion of one centered site. Difference Fourier maps normal to and at the midpoint of the Cr–Cr axis were calculated without the H/D atom in order to investigate this disorder and are illustrated in parts A and B of Figure 1. The nuclear density contours within these Fourier cross sections are elongated along directions somewhat staggered with respect to the four Cr–CO(eq) directions. Because of the H atom's greater nuclear thermal motion at room temperature, this effect is more pronounced in Figure 1A.

Although detailed information about the exact nature of this disorder is limited inherently by the available resolution, several conclusions can be drawn. First, the D atom's disorder must be greater than that observed for the $[Et_4N]^+$ salt. For a twofold disordered model a difference Fourier nuclear density map (calculated without the μ-D atom) would exhibit a dumbbell shape, which is distinctly different from the contour map shapes in Figure 1A,B. Since the resolution of our 17 K neutron data and the room-temperature data for the $[Et_4N]^+$ salt are comparable (i.e., a maximum (sin θ)/λ of ca. 0.70 Å^{-1}), one should expect to be able to resolve a similar twofold site distribution (with a separation of 0.6 Å) if it were present in the

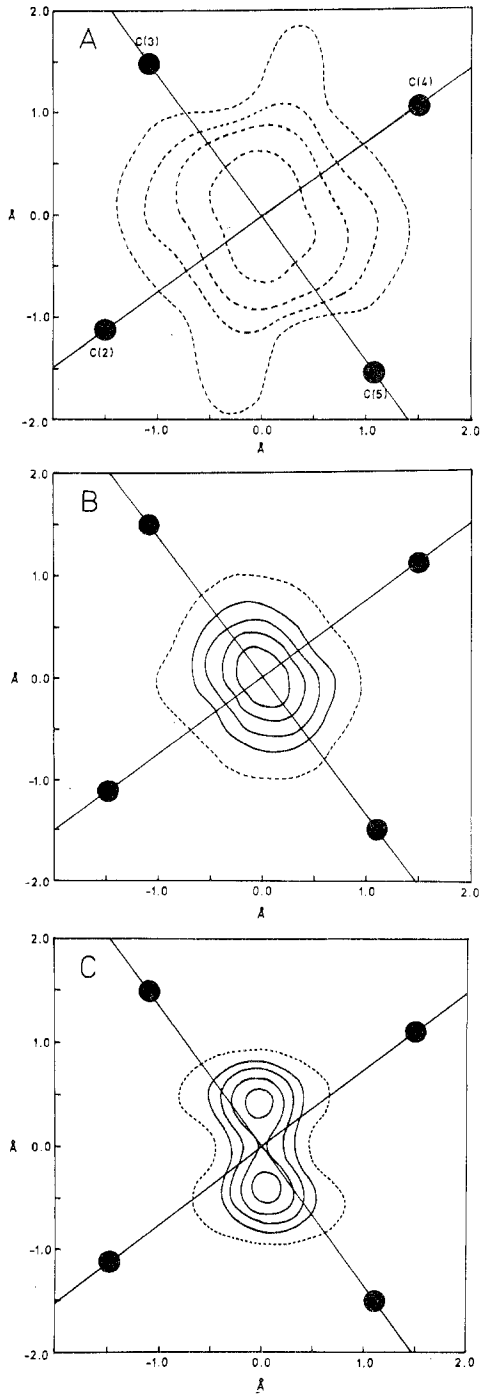

Figure 1. Contoured difference Fourier nuclear density maps for the plane normal to the Cr–Cr axis and passing through the midpoint of the Cr–Cr line. The positions of the axial carbon atoms of the monoanion are projected on the contour maps and represented by the darkened circles. (A) Room-temperature neutron diffraction data for $[(Ph_3P)_2N]^+[Cr_2(CO)_{10}(\mu\text{-H})]^-$ without the inclusion of the bridging H atom. Dashed contours are drawn at 0.0, −0.1, −0.2, and −0.4. (B) Low-temperature neutron diffraction data for $[(Ph_3P)_2N]^+[Cr_2(CO)_{10}(\mu\text{-D})]^-$ without inclusion of the bridging D atom. Contours are drawn at 0.0 (dashed), 0.8, 1.2, 1.6, and 2.0. (C) Low-temperature data with the inclusion of only one of the two independent disordered sites displaced 0.3 Å from the Cr–Cr line.

$[(Ph_3P)_2N]^+$ salt. Second, the sterically preferred staggered location of the μ-H atom in the $[Et_4N]^+$ salt suggests a similar arrangement for the disordered sites may exist in the $[(Ph_3P)_2N]^+$ salt. However, since the eclipsed geometry of the anion provides four equivalent sites in the latter, we assume each is equally populated.

To evaluate whether or not our neutron data would accommodate a fourfold site distribution, we initiated another least-squares refine-

Table II. Positional and Thermal Parameters for the $[Cr_2(CO)_{10}(\mu\text{-}D)]^-$ Monoanion and Root-Mean-Square Thermal Displacements (Å) of Atoms along Their Principal Axes (17 K)[a-d]

atom	10^5x	10^5y	10^5z	$10^5\beta_{11}$	$10^5\beta_{22}$	$10^5\beta_{33}$	$10^5\beta_{12}$	$10^5\beta_{13}$	$10^5\beta_{23}$	$10^3u(1)$	$10^3u(2)$	$10^3u(3)$
Cr	6278 (11)	2231 (12)	13241 (14)	37 (6)	17 (6)	28 (10)	−2 (5)	12 (7)	0 (6)	45 (8)	47 (9)	87 (12)
	6277 (11)	2225 (12)	13241 (14)	38 (6)	18 (6)	33 (10)	−3 (5)	14 (7)	1 (6)			
C(1)	13046 (6)	3978 (7)	27797 (8)	54 (3)	85 (4)	64 (6)	0 (3)	26 (4)	−13 (4)	69 (2)	97 (5)	109 (4)
	13048 (6)	3977 (7)	27797 (8)	54 (3)	85 (4)	64 (6)	0 (3)	26 (4)	−12 (4)			
O(1)	17371 (8)	5120 (9)	36956 (10)	78 (4)	126 (5)	64 (7)	1 (4)	21 (5)	−22 (5)	68 (4)	120 (4)	137 (5)
	17371 (8)	5121 (9)	36956 (10)	78 (4)	126 (5)	65 (7)	2 (4)	21 (5)	−20 (5)			
C(2)	10430 (7)	11624 (7)	10772 (9)	75 (4)	66 (4)	134 (6)	−10 (3)	70 (4)	−3 (4)	85 (6)	97 (5)	107 (2)
	10431 (7)	11625 (7)	10771 (9)	76 (4)	66 (4)	134 (6)	−9 (3)	70 (4)	−3 (4)			
O(2)	13061 (8)	17308 (8)	9479 (11)	128 (5)	69 (5)	236 (8)	−20 (4)	129 (5)	7 (5)	80 (7)	122 (6)	141 (2)
	13063 (8)	17309 (8)	9479 (11)	129 (5)	69 (5)	239 (8)	−20 (4)	131 (5)	7 (5)			
C(3)	−1660 (6)	9432 (7)	11545 (9)	51 (3)	79 (4)	133 (6)	5 (3)	50 (4)	4 (4)	82 (4)	102 (3)	106 (4)
	−1661 (6)	9430 (7)	11544 (9)	51 (3)	79 (4)	133 (6)	5 (3)	50 (4)	6 (4)			
O(3)	−6176 (8)	13983 (8)	10652 (11)	93 (5)	88 (5)	243 (8)	31 (4)	106 (5)	40 (5)	88 (5)	112 (7)	145 (2)
	−6174 (8)	13981 (8)	10652 (11)	92 (4)	88 (5)	243 (8)	31 (4)	105 (5)	40 (5)			
C(4)	1742 (7)	−7404 (7)	14606 (9)	70 (4)	57 (4)	114 (6)	0 (3)	56 (4)	12 (4)	80 (4)	98 (4)	100 (4)
	1742 (6)	−7405 (7)	14606 (8)	70 (4)	56 (4)	114 (6)	1 (3)	56 (4)	12 (4)			
O(4)	−889 (8)	−13378 (8)	15351 (11)	115 (5)	65 (5)	188 (8)	−17 (4)	102 (5)	5 (5)	82 (6)	117 (6)	130 (3)
	−888 (8)	−13376 (8)	15351 (10)	115 (5)	65 (5)	187 (8)	−18 (4)	101 (5)	4 (5)			
C(5)	14097 (7)	−4429 (7)	14194 (9)	67 (4)	90 (4)	139 (6)	−3 (3)	65 (4)	−16 (4)	89 (8)	99 (2)	114 (3)
	14095 (7)	−4428 (7)	14192 (9)	66 (4)	90 (4)	139 (6)	−3 (3)	65 (4)	−17 (4)			
O(5)	18971 (8)	−8327 (9)	14962 (11)	90 (4)	110 (5)	215 (8)	31 (4)	97 (5)	−1 (5)	82 (8)	131 (2)	134 (4)
	18971 (8)	−8325 (9)	14961 (11)	93 (4)	111 (5)	218 (8)	30 (4)	101 (5)	−3 (5)			
D(1)	471	2022 (68)	−631 (68)	$B = 1.5$ (2) Å^2								
D(2)	−1886 (66)	275 (67)	−81 (70)	$B = 1.6$ (2) Å^2								
D	0	0	0	730 (28)	836 (31)	254 (21)	−291 (24)	176 (20)	−233 (21)	119 (8)	304 (10)	404 (8)

[a] For each atom in the monoanion, the parameters from the refinement of the fourfold disordered model are given above the corresponding results from the anisotropic refinement. For the two refinements the corresponding parameters for the nondeuterium atoms agree within 1 esd. [b] The estimated standard deviations in parentheses for this and all subsequent tables refer to the least significant digits. [c] The parameters for the $[(Ph_3P)_2N]^+$ cation are available as supplementary material. [d] The form of the anisotropic temperature factor is $\exp\{-(\beta_{11}h^2 + \beta_{22}k^2 + \beta_{33}l^2 + 2\beta_{12}hk + 2\beta_{13}hl + 2\beta_{23}kl)\}$.

ment with the one centered D atom position replaced by a fourfold disordered site model. Idealized staggered positions of the two independent D atom sites ($x_1 = 0.0045$, $y_1 = 0.0181$, $z_1 = 0.0043$; $x_2 = -0.0133$, $y_2 = -0.0032$, $z_2 = 0.0015$) displaced 0.3 Å from the crystallographic center of symmetry were calculated with MIRAGE.[15] The close proximity of the four sites, however, makes the refinement extremely difficult. Whereas the symmetry-related sites are separated by 0.6 Å, the neighboring independent sites are separated by only ca. 0.4 Å. Although at 17 K the μ-D atom's thermal motion is primarily due to zero-point energy, its magnitude is sufficient to prevent the observation of the individual sites in a difference Fourier map. A reasonable minimum estimate of the averaged thermal displacement for an individual site is $u(1)$ for the μ-D atom (anisotropic refinement), which represents a thermal displacement of 0.12 Å along the Cr–Cr line. Consequently, since this displacement is relatively large compared to the site separation, contributions from each site (enclosed by the anisotropic thermal ellipsoid) overlap to produce the composite peak at the center of symmetry.

Refinement[16] was begun with each quarter-weighted deuterium site assigned a B_{iso} of 2.0 Å^2 while the $[(Ph_3P)_2N]^+$ cation parameters were held fixed. After two least-squares cycles only the positional parameters for the two D sites continued to vary. A broad and rather poorly defined convergence minimum was indicated (for μ-D) and was characterized by a large correlation coefficient (0.85) between the x coordinate for D(1) and the y coordinate for D(2). However, the corresponding Cr–D separations, Cr–D–Cr bond angles, and the calculated discrepancy indices remained unchanged. During subsequent refinement cycles only the x coordinate for D(1) was held fixed. The average D scattering length in the disordered model was then redetermined (0.480×10^{-12} cm). Full-matrix least-squares refinement of the fourfold disordered model led to the discrepancy indices in Table I.[17] Subsequent Fourier maps of the anisotropic and disordered models both placed the μ-D atom nuclear density maximum at exactly $x = 0.0$, $y = 0.0$, and $z = 0.0$. The magnitudes of the peak maxima were equal within experimental error. The corresponding difference Fourier maps show no unusual features in the vicinity of the center of symmetry. An additional difference Fourier map (shown in Figure 1C) was calculated without the inclusion of the second D atom site to verify its position. The contour map clearly resolves the approximate position[18] of the second independent site which is staggered with respect to the four Cr–CO(eq) directions. The dumbbell shape arises due to the overlap of the two closely spaced, symmetry-related positions.

Table III. Internuclear Distances (Å) and Bond Angles (deg) for the $[(Cr_2(CO)_{10}(\mu\text{-}D)]^-$ Monoanion from the Refinement of the Fourfold Disordered Model[a,b]

(A) Internuclear Separations

Cr–Cr′	3.390 (3)		
Cr–D(1)	1.737 (9)	Cr–D(2)	1.750 (8)
Cr′–D(1)	1.718 (9)	Cr′–D(2)	1.729 (11)
Cr–C(1)	1.841 (2)	C(1)–O(1)	1.160 (2)
Cr–C(2)	1.899 (3)	C(2)–O(2)	1.148 (2)
Cr–C(3)	1.915 (3)	C(3)–O(3)	1.139 (2)
Cr–C(4)	1.897 (3)	C(4)–O(4)	1.148 (2)
Cr–C(5)	1.894 (3)	C(5)–O(5)	1.146 (2)

(B) Bond Angles

Cr–D(1)–Cr′	157.6 (7)	Cr–D(2)–Cr′	153.9 (10)
D(1)–Cr–C(1)	165.4 (4)	D(2)–Cr–C(1)	166.8 (5)
D(1)–Cr–C(2)	99.6 (5)	D(2)–Cr–C(2)	97.7 (4)
D(1)–Cr–C(3)	97.7 (5)	D(2)–Cr–C(3)	78.8 (5)
D(1)–Cr–C(4)	76.0 (5)	D(2)–Cr–C(4)	78.3 (4)
D(1)–Cr–C(5)	80.7 (5)	D(2)–Cr–C(5)	99.5 (4)
Cr–C(1)–O(1)	179.2 (2)	C(1)–Cr–C(5)	90.8 (1)
Cr–C(2)–O(2)	178.7 (1)	C(2)–Cr–C(3)	88.3 (1)
Cr–C(3)–O(3)	177.2 (1)	C(2)–Cr–C(4)	175.6 (1)
Cr–C(4)–O(4)	178.0 (2)	C(2)–Cr–C(5)	88.3 (1)
Cr–C(5)–O(5)	178.3 (1)	C(3)–Cr–C(4)	92.5 (1)
C(1)–Cr–C(2)	91.9 (1)	C(3)–Cr–C(5)	176.0 (2)
C(1)–Cr–C(3)	91.6 (1)	C(4)–Cr–C(5)	90.6 (1)
C(1)–Cr–C(4)	92.4 (1)		

[a] The esd's in parentheses for the internuclear separations and bond angles were calculated from the standard errors of the fractional coordinates for the corresponding atomic positions. [b] The corresponding structural parameters for the $[(Ph_3P)_2N]^+$ are available as supplementary material.

The final positional and thermal parameters for the anion from both refinements are presented in Table II. Selected internuclear distances and bond angles with esd's calculated from the variance–covariance matrix are given in Table III. Structure factor tables and the refined parameters associated with the $[(Ph_3P)_2N]^+$ cation are available as supplementary material. The computer programs used, with their accession names in the World List of Crystallographic Computer Programs (3rd ed.), are as follows: absorption correction,

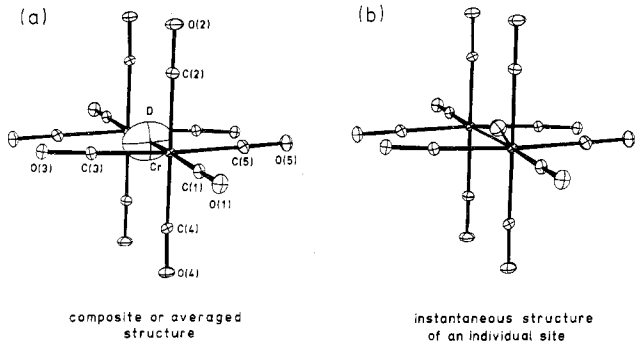

Figure 2. Molecular configuration of the $[Cr_2(CO)_{10}(\mu\text{-D})]^-$ monoanion observed at 17 K depicting (a) the composite or averaged eclipsed structure and (b) the instantaneous C_{2v}-$mm2$ structure with the bridging D atom displaced ca. 0.3 Å from the Cr–Cr line in a "closed" Cr–D–Cr bond.[6] Thermal ellipsoids were scaled to enclose 50% probability.

ABSOR;[19] data averaging and sorting, DATASORT; Fourier summation, CNTFOR (modification of FORDAP); least-squares refinements, ORXFLS3; error analysis of distances and angles, ORFFE3; structural drawings, ORTEPII. Least-squares planes of interest are provided in Table IV.[20,21]

Results and Discussion

Description of the Molecular Structure of $[Cr_2(CO)_{10}(\mu\text{-D})]^-$. The crystal structure of the $[Cr_2(CO)_{10}(\mu\text{-D})]^-$ monoanion is illustrated in Figure 2a. The anion conforms closely to an idealized D_{4h} geometry with the bridging D atom disposed symmetrically between the two Cr atoms. Since the CO group trans to the bridging D atom is a better electron acceptor, π back-donation from filled Cr metal orbitals to the π^* antibonding CO orbitals reduces the Cr–C(1) separation to 1.841 (2) Å and increases the C(1)–O(1) distance to 1.160 (2) Å from the averaged values of 1.901 (4) and 1.145 (2) Å, respectively, for the remaining four equatorial carbonyl groups.

Our structural investigations[3] of the $[Cr_2(CO)_{10}(\mu\text{-H})]^-$ monoanion have allowed examination of the effects of crystal packing forces on the molecular structure. Despite the similarly eclipsed metal carbonyl framework for the $[Et_4N]^+$ and $[(Ph_3P)_2N]^+$ salts, several significant differences exist. For the $[Et_4N]^+$ salt a twofold disorder of the off-axis hydrogen position was indicated. Although the corresponding disorder of the nonhydrogen atoms is not resolved, it is reflected by the size, shape, and orientation of the thermal ellipsoids of the axial CO group trans to the bridging H atom. An analysis of the root-mean-square thermal displacements for the axial carbonyl atoms provides strong evidence that the observed nonhydrogen structure is a composite of two slightly bent, identical $[Cr_2(CO)_{10}(\mu\text{-H})]^-$ monoanions of C_{2v}-$mm2$ geometry. A similar structure has been observed by Bau and co-workers[4,22] in $[Et_4N]^+[W_2(CO)_{10}(\mu\text{-H})]^-$ at 14 K. For several of the carbonyl atoms in the tungsten species, the disorder has actually been resolved. This distortion of the metal carbonyl framework reduces the number of off-axis staggered sites from four equivalent positions in the idealized D_{4h} structure to one favored position in the bent C_{2v} structure. The observed anion structure still retains an overall D_{4h} configuration, however, since the half-weighted C and O atoms are displaced ca. 0.1–0.2 Å from their respective neutron-determined composite positions. In contrast, for the $[(Ph_3P)_2N]^+$ salt, the nonhydrogen backbone of the anion is completely ordered down to 17 K. The positions of the nonhydrogen atoms are determined with a high degree of precision and their thermal parameters provide no indication of a structural disorder. The D_{4h} symmetry of the metal carbonyl framework is strictly maintained and the μ-H/D atom in this case appears to be disordered among at least four off-axis sites. Thus, a comparison of the crystal structures of the two salts establishes that packing forces modify the geometry of the $[Cr_2(CO)_{10}(\mu\text{-H})]^-$ anion.

Table IV. Equations of "Best" Least-Squares Planes, Perpendicular Distances (Å) from these Planes, and Dihedral Angles between the Planes[a-c]

(A) Plane I through Cr, Cr′, D(1), and D(1)′

$21.0033x + 1.6919y - 10.2436z = 0$

Cr	0.001 (3)	Cr′	−0.001 (3)
D(1)	0.001 (16)	D(1)′	0.001 (3)
D(2)	−0.384 (16)	D(2)′	0.384 (16)
C(1)	−0.040 (2)	O(1)	−0.051 (2)
C(2)	1.284 (2)	O(2)	2.066 (2)
C(3)	−1.372 (2)	O(3)	−2.152 (2)
C(4)	−1.256 (2)	O(4)	−1.986 (2)
C(5)	1.432 (2)	O(5)	2.311 (2)

(B) Plane II through Cr, Cr′, D(2), and D(2)′

$2.4547x + 15.5309y - 3.7666z = 0$

Cr	−0.001 (2)	Cr′	0.001 (2)
D(1)	0.327 (11)	D(1)′	−0.327 (11)
D(2)	0.001 (11)	D(2)′	−0.001 (11)
C(1)	−0.113 (2)	O(1)	−0.176 (2)
C(2)	1.653 (2)	O(2)	2.648 (2)
C(3)	0.990 (2)	O(3)	1.621 (2)
C(4)	−1.658 (2)	O(4)	−2.678 (2)
C(5)	−0.881 (2)	O(5)	−1.397 (2)

(C) Plane III through Cr, C(2), C(3), C(4), and C(5)

$-0.0806x - 2.4432y - 12.3210z + 1.6410 = 0$

Cr	−0.051 (2)	Cr′	3.333 (2)
D(1)	1.670 (9)	D(1)′	1.613 (9)
D(2)	1.646 (9)	D(2)′	1.637 (9)
C(1)	−1.892 (2)	O(1)	−3.052 (2)
C(2)	0.022 (2)	O(2)	0.040 (2)
C(3)	−0.011 (2)	O(3)	−0.009 (2)
C(4)	0.021 (2)	O(4)	0.078 (2)
C(5)	−0.012 (2)	O(5)	−0.015 (2)

(D) Plane IV through Cr, Cr′, C(1), C(2), and C(4)

$-17.1927x + 9.2003y + 6.7174x + 0.0030 = 0$

Cr	0.019 (3)	Cr′	−0.013 (2)
D(1)	0.228 (15)	D(1)′	−0.222 (15)
D(2)	0.348 (15)	D(2)′	−0.342 (15)
C(1)	−0.007 (2)	O(1)	−0.031 (2)
C(2)	0.003 (2)	O(2)	−0.014 (2)
C(3)	1.932 (2)	O(3)	3.067 (2)
C(4)	0.004 (2)	O(4)	−0.044 (2)
C(5)	−1.875 (2)	O(5)	−3.020 (2)

(E) Plane V through Cr, Cr′, C(1), C(3), and C(5)

$12.4873x + 12.6675y - 7.6919z - 0.0527 = 0$

Cr	−0.005 (3)	Cr′	−0.101 (3)
D(1)	0.194 (13)	D(1)′	−0.299 (13)
D(2)	−0.248 (13)	D(2)′	0.142 (13)
C(1)	−0.058 (2)	O(1)	−0.078 (2)
C(2)	1.894 (2)	O(2)	3.042 (2)
C(3)	0.047 (2)	O(3)	0.129 (2)
C(4)	−1.897 (2)	O(4)	−3.040 (2)
C(5)	−0.055 (2)	O(5)	0.111 (2)

Dihedral Angles (deg) between Planes

planes	angle	planes	angle
I and II	76.9	II and IV	42.1
I and III	86.5	II and V	47.3
I and IV	61.0	III and IV	89.6
I and V	29.6	III and V	88.1
II and III	88.3	IV and V	89.4

[a] The equations of the least-squares planes are expressed in terms of monoclinic fractional coordinates x, y, and z. [b] The atomic positions used in the calculation for a given plane were weighted according to their estimated errors. [c] The primed atom is related by the center of symmetry at the origin.

Although these subtle differences are substantially smaller than those observed for the Mo[23,24] and W[25] analogues, they do influence the configuration of the M–H–M bond in these systems.

The large thermal ellipsoid for the bridging D atom, relative to those of the remaining nonhydrogen atoms, clearly repre-

sents the most unusual feature of this structural analysis. Even though the thermal parameters for the ordered nonhydrogen atoms decrease proportionally with decreased temperature, the corresponding parameters for the bridging D atom remain essentially unaffected. These results strongly support a disordered D atom configuration for the $[(Ph_3P)_2N]^+$ salt.

Fourfold Disorder of the Bridging Hydrogen Position. As clearly depicted in Figure 2a the extremely large thermal ellipsoid for the bridging D atom is not consistent with a completely ordered monoanion. The "averaged" structure in Figure 2a represents a superposition of several deuterium nuclear sites, and the D atom's large thermal displacements in the plane normal to the Cr–Cr bond line[26] indicate a site occupation distribution within this plane. A refinement of a fourfold disorder of the off-axis D atom positions (which are staggered with respect to the four Cr–CO(eq) directions) has led to a reasonable agreement. The Cr–D–Cr bond distances and angles are comparable to those[27] in the $[Et_4N]^+$ salt, in which the off-axis H atom position was resolved. The dihedral angles between the two independent Cr–D–Cr planes as well as the two mean planes through the two Cr atoms and the two axial and four equatorial CO ligands are near 45° (see Table IV). Thus this refinement supports the anion's structure for an individual D site presented in Figure 2b, which depicts the presence of a closed-type Cr–D–Cr bond.

Although the neutron diffraction experiment provides an averaged (Figure 2a), rather than an instantaneous representation (Figure 2b) of the anion's structure, the disordered bridging D atom configuration suggests that the potential energy well for each D site may be relatively shallow. Depending upon the magnitude of the barrier to interconversion, the observed structure may indicate a dynamic rather than a static disorder. This is strongly supported by the completely ordered structure for the anion's nonhydrogen backbone in the $[(Ph_3P)_2N]^+$ salt. Temperature-dependent solid-state NMR measurements are needed to characterize further the nature of the disorder.

Finally, in both of the salts, the anion is constrained to lie on a crystallographic center of symmetry. While this reduces the size of the structural refinement, it makes the interpretation less straightforward.[28] To eliminate this problem, we are preparing other salts with the hope of finding one in which the anion's structure is not constrained crystallographically. The problem which remains to be addressed is whether the anion prefers in the absence of site symmetry a slightly bent structure with one off-axis bridging H atom position or a D_{4h} structure accompanied by a fourfold disordered H atom configuration.

Acknowledgment. This collaborative study is based upon work partially supported by the National Science Foundation under Project No. CHE78-20698 (to J.M.W.).[1] Computer time for the refinement of the low-temperature neutron data was provided to J.L.P. by the West Virginia Network for Educational Telecomputing. The authors also extend their appreciation to Professor L. F. Dahl for his helpful discussions and continued interest in this project.

Registry No. $[(Ph_3P)_2N]^+[Cr_2(CO)_{10}(\mu\text{-}D)]^-$, 71661-63-7.

Supplementary Material Available: Listings of structure factor amplitudes, positional and thermal parameters, and bond distances and angles (23 pages). Ordering information is given on any current masthead page.

References and Notes

(1) This work was performed under the auspices of the Division of Basic Energy Sciences of the U.S. Department of Energy.
(2) (a) West Virginia University. (b) Argonne National Laboratory. (c) Brookhaven National Laboratory; research collaborator from Argonne National Laboratory. (d) Brookhaven National Laboratory.
(3) (a) J. Roziere, J. M. Williams, R. P. Stewart, Jr., J. L. Petersen, and L. F Dahl, *J. Am. Chem. Soc.*, **99**, 4497 (1977); (b) J. L. Petersen, P. L. Johnson, J. O'Connor, L. F. Dahl, and J. M. Williams, *Inorg. Chem.*, **17**, 3460 (1978); (c) J. L. Petersen, L. F. Dahl, and J. M. Williams, *Adv. Chem. Ser.*, **No. 167**, 11 (1978).
(4) (a) R. Bau, R. G. Teller, S. W. Kirtley, and T. F. Koetzle, *Acc. Chem. Res.*, **12**, 176 (1979); (b) R. Bau and T. F. Koetzle, *Pure Appl. Chem.*, **50**, 55 (1978).
(5) D. J. Darensbourg and M. J. Incorvia, *Inorg. Chem.*, **18**, 18 (1979), and references cited therein.
(6) In a "closed-type" M–H–M bond the overlap region in the bond is displaced from the H atom. This type of three-center, two-electron bond is represented formally by

which suggests that it contains a substantial metal–metal bonding component.
(7) (a) L. B. Handy, P. M. Treichel, L. F. Dahl, and R. G. Hayter, *J. Am. Chem. Soc.*, **88**, 366 (1966); (b) L. B. Handy, J. K. Ruff, and L. F. Dahl, *ibid.*, **92**, 7312 (1970).
(8) R. G. Hayter, *J. Am. Chem. Soc.*, **88**, 4376 (1966).
(9) $R(F_o) = [\sum||F_o| - |F_c||/\sum|F_o|]$, $R(F_o^2) = \sum|F_o^2 - F_c^2|/\sum F_o^2$, and $R_w(F_o^2) = [\sum w_i|F_o^2 - F_c^2|^2/\sum w_i F_o^4]^{1/2}$. All least-squares refinements of the neutron data were based on the minimization of $\sum w_i|F_o^2 - S^2F_c^2|^2$ with individual weights $w_i = 1/\sigma^2(F_o^2)$.
(10) The Zachariasen approximation[11] was used for the overall isotropic g parameter as defined and scaled by Coppens and Hamilton.[12] The F_o values were corrected for extinction from the expression $|F_o|_{corr} = |F_o|(1 + \bar{T}2g\lambda^3|F_c|^2/V^2 \sin 2\theta)^{-1/4}$, where $|F_c|$ is on an absolute scale, λ is the wavelength (Å), g is the refined extinction parameter, $\bar{T}$ is the mean absorption-weighted path length in the crystal in centimeters (calculated simultaneously during the computation of absorption corrections), and V is the unit cell volume (Å^3).
(11) W. H. Zachariasen, *Acta Crystallogr.*, **23**, 558 (1967).
(12) P. Coppens and W. C. Hamilton, *Acta Crystallogr., Sect. A*, **26**, 71 (1970).
(13) The neutron scattering lengths used[14] in this study were $\bar{b}_{Cr} = 0.352$, $\bar{b}_N = 0.940$, $\bar{b}_P = 0.510$, $\bar{b}_C = 0.663$, $\bar{b}_O = 0.575$, and $\bar{b}_H = -0.372$ (all units in 10^{-12} cm).
(14) G. E. Bacon, *Acta Crystallogr., Sect. A*, **28**, 357 (1972).
(15) J. C. Calabrese, MIRAGE, Ph.D. Thesis (Appendix III), University of Wisconsin—Madison, 1971.
(16) The close proximity of the disordered sites prohibits an anisotropic refinement of the off-axis D sites. Looking back at our analysis[3b] of the room-temperature data, the anisotropic refinement of the averaged H structure was inadequate since it cannot take into account the additional nuclear density features present in the difference Fourier map (Figure 1A) for the bridging H atom. The inherent nature of the three by three tensor associated with the anisotropic equation has the effect of averaging out these features during the refinement. Although the shape of the thermal ellipsoid for the bridging D atom is rather meaningless under these circumstances, its size and orientation do reflect the magnitude and direction of the disorder. Since a distinct off-axis position was resolved at room temperature for the bridging H atom in the $[Et_4N]^+$ salt, an anisotropic refinement was possible. In the $[(Ph_3P)_2N]^+$ salt the "averaged" result prohibits the observation of the individual sites and thereby forces one to initiate the refinement with idealized coordinates and use an isotropic thermal model for the analysis. Although the resolution of the difference Fourier map in Figure 1B may not appear to support the refinement of the disordered model, generally for situations involving a disordered site distribution the resolution in a Fourier map can be considerably less than what is required to obtain from a least-squares analysis meaningful values for the refined parameters. Whereas the room-temperature neutron data ($(\sin\theta)/\lambda$ maximum of 0.5 Å^{-1}) for the $[(Ph_3P)_2N]^+$ salt clearly did not permit the refinement of a disordered μ-H atom structure, the conditions are more favorable here due to the much lower temperature and larger data set.
(17) A least-squares refinement was also attempted with an eclipsed rather than staggered arrangement of the disordered D sites. However, during several cycles of refinement the coordinates of the eclipsed positions varied considerably and moved toward the coordinates of the preferred staggered positions.
(18) The interpolated coordinates of the second site, D2, were $x = -0.019$, $y = 0.003$, and $z = -0.001$ which compare relatively well with the refined coordinates in Table II.
(19) A modification of an analytical method developed by J. de Meulenaer and H. Tompa, *Acta. Crystallogr.*, **19**, 1014 (1965).
(20) For the determination of the "best" equation for each least-squares plane and the perpendicular distances of atoms from the plane, the program PLNJO was employed.[21]
(21) J. O. Lundgren, University of Uppsala, Uppsala, Sweden; based on the method of D. Blow, *Acta Crystallogr.*, **16**, 168 (1960).
(22) D. W. Hart, R. Bau, and T. F. Koetzle, submitted for publication.
(23) For the $[Et_4N]^+$ aand $[(Ph_3P)_2N]^+$ salts, the metal carbonyl framework of the $[Mo_2(CO)_{10}(\mu\text{-}H)]^-$ anion is analogous[24] to that found for the tungsten species.[25] In the $[Et_4N]^+$ salt a linear, eclipsed metal carbonyl structure exists, whereas for the $[(Ph_3P)_2N]^+$ salt a bent, staggered carbonyl configuration is observed with the metal–metal separation being ca. 0.1 Å less in the bent form.

(24) J. L. Petersen and R. P. Stewart, Jr., unpublished research.
(25) R. D. Wilson, S. A. Graham, and R. Bau, *J. Organomet. Chem.*, **91**, C49 (1975).
(26) The root-mean-square thermal displacements of $u(2) = 0.304$ (10) Å and $u(3) = 0.404$ (8) Å obtained from the anisotropic refinement of the bridging D atom are directed 91 (2) and 92 (1)°, respectively, with respect to the Cr–Cr line.
(27) In the $[Et_4N]^+$ salt, the Cr–H–Cr bond angle is 158.9 (6)° and the two independent Cr–H internuclear separations are 1.707 (21) and 1.737 (19) Å.
(28) J. L. Petersen, L. F. Dahl, and J. M. Williams, *J. Am. Chem. Soc.*, **96**, 6610 (1974), and references cited therein.

Contribution from the Department of Chemistry, University of Kansas, Lawrence, Kansas 66045, and Xerox Corporation, Webster Research Center, Webster, New York 14580

The Nature of Triphenylselenonium Chloride. Crystal and Molecular Structure of the Monohydrate: $(C_6H_5)_3SeCl·H_2O$

RENONIA V. MITCHAM,[1a] BYUNGKOOK LEE,*[1a] KRISTIN BOWMAN MERTES,[1a] and RONALD F. ZIOLO*[1b]

Received May 14, 1979

Triphenylselenonium chloride hydrate ($(C_6H_5)_3SeCl·H_2O$), previously reported to be anhydrous, has been synthesized and investigated via a full three-dimensional X-ray structural analysis. The salt crystallizes in the noncentrosymmetric orthorhombic space group $Pna2_1$ with $a = 10.974$ (2) Å, $b = 10.444$ (4) Å, and $c = 14.493$ (4) Å (22 °C); $V = 1661.1$ (8) Å^3, $Z = 4$, $d_{calcd} = 1.454$ g/cm^3, and $d_{obsd} = 1.46$ (2) g/cm^3. Diffraction data were collected with a Syntex $P2_1$ diffractometer using graphite-monochromated Mo Kα radiation. The structure was solved by the heavy-atom technique and refined by full-matrix least-squares methods using 2001 symmetry-independent reflections. Anisotropic thermal motion was assumed for all nonhydrogen atoms. The resulting discrepancy indicies are $R_F = 0.037$ and $R_{wF} = 0.029$. The structure consists of triphenylselenonium cations, chloride ions, and water molecules linked by a secondary bonding scheme involving shorter than van der Waals Se–Cl (3.530 (2) Å) and Se–O (3.147 (4) Å) distances. The salt is monomeric (Se–Se: 7.414 (2) Å) with five-coordinate selenium and has a packing arrangement different from that of the six-coordinate, dimeric dihydrate, $(C_6H_5)_3SeCl·2H_2O$. Enantiomorphs of the triphenylselenonium ion alternate along a hydrogen-bonded water–chlorine chain that runs parallel to a at $y = {}^1/_4$, $z = 0$ and $y = {}^3/_4$, $z = {}^1/_2$. The spatial arrangement of the five-coordination sites in the monohydrate is nearly identical with that in the dihydrate providing strong evidence that the Se–Cl and Se–O interactions are directed, albeit weak, chemical bonds. Additionally, shorter Se–Cl and Se–O distances are observed in the monohydrate, consistent with the lower coordination number for selenium. These salts constitute the first examples of two distinctly different group 6 onium-salt compounds that possess directly comparable secondary interactions. Calculated X-ray powder patterns are provided for identification and comparison of the monohydrate and dihydrate which constitute the only two characterized forms of $(C_6H_5)_3SeCl$. Numerous attemps to obtain the anhydrous salt by slow, open-air solvent evaporation resulted in the formation of only hydrated or solvated crystals. Discussion on the crystallization and characterization of the salt is given, and the existence of an anhydrous form under ordinary conditions is questioned. Triphenylselenonium chloride demonstrates a high propensity for water.

Introduction

Secondary bonding has been shown to play a central role in the structures of the triorganoselenonium and triorganotelluronium salts.[2-4] Recently, Lee and Titus reported the X-ray structure of triphenylselenonium chloride dihydrate, $(C_6H_5)_3SeCl·2H_2O$, and showed that both water molecules and chloride ion formed a contiguous part of the structure by being involved in a secondary bonding scheme with the selenium atom.[5] The compound is dimeric (Se–Se: 4.762 (8) Å) with bridging chloride ions and one water molecule contributing to form six-coordinate selenium. Since 1929, the dihydrate and a so-called "anhydrous" compound have constituted the only known forms of triphenylselenonium chloride.[6]

In an early X-ray study of the "anhydrous" form, McCullough and Marsh were able to determine the atomic positional parameters of the selenium and chlorine atoms.[7] In this form the shortest Se–Cl distance (3.67 Å)[8] is approximately equal to the sum of the respective van der Waals radii, 3.65 Å, which suggests the absence of secondary bonding between selenium and chlorine.[9] Furthermore, the shortest Se–Se distance (7.51 Å) rules out a dimeric structure and suggests that selenium is three-coordinate which would be unlikely in view of the potential donor capacity of the chloride ion.[10] To resolve this situation, we determined the complete X-ray structure of triphenylselenonium chloride.

Experimental Section

Crystal Preparation and Data. Crude triphenylselenonium chloride was obtained from ROC/RIC Corp., Sun Valley, Calif. Several grams were purified by extracting an aqueous solution three times with reagent grade benzene and passing it down a column containing purified Dowex 1-X8 (100–200 mesh) ion-exchange resin. The resulting clear, colorless solution was vacuum evaporated at about 60 °C until crystals appeared. The solution was then cooled and filtered to remove the crystallized salt which was subsequently dried in a vacuum desiccator. Crystals suitable for X-ray diffraction studies were obtained by slow, open evaporation of a 60:40 v/v mixture of methylene chloride and ethyl acetate containing about 5 wt % $(C_6H_5)_3SeCl$. The solvent mixture was dried with anhydrous $MgSO_4$ before use. During evaporation, the room temperature was 23 °C and the relative humidity about 60%.

Preliminary precession photographs showed extinctions ($0kl$, $k + l \neq 2n$; $h0l$, $h \neq 2n$) consistent with the orthorhombic space groups $Pnam$ and $Pna2_1$. Accurate cell dimensions were calculated by using a least-squares procedure to fit the orientation angles of 15 randomly chosen reflections measured on a Syntex $P2_1$ diffractometer. The density, 1.46 (2) g/cm^3, was measured by flotation in a mixture of hexane and CCl_4 and was consistent with 4 formula units/unit cell. The noncentrosymmetric space group $Pna2_1$ was assumed since mirror or inversion center symmetry was unlikely for $(C_6H_5)_3SeCl$. This assignment was later confirmed by the Patterson map and by the successful refinement of the structure. Crystal data are as follows: $a = 10.974$ (2) Å, $b = 10.444$ (4) Å, $c = 14.493$ (4) Å, $V = 1661.1$ (8) Å^3, and $Z = 4$. The space group and cell dimensions appeared identical with those reported for anhydrous $(C_6H_5)_3SeCl$.[7] Better agreement between the observed and calculated densities, however, was obtained by assuming the presence of one water molecule: d_{calcd} ($(C_6H_5)_3SeCl·H_2O$) = 1.454 g/cm^3 vs. d_{calcd} ($(C_6H_5)_3SeCl$) = 1.382 g/cm^3. Subsequent electron density maps and thermal gravimetric data confirmed the presence and amount of H_2O. The linear absorption coefficient, μ(Mo Kα) ($\lambda = 0.710\,688$ Å), and $F(000)$ for $(C_6H_5)_3SeCl·H_2O$ (mol wt 363.75) are 27.0 cm^{-1} and 736, respectively.

X-ray powder diffraction patterns were calculated by using Clark, Smith, and Johnson's POWD5.[11] Atomic positional and thermal parameters (anisotropic for nonhydrogen and isotropic for hydrogen atoms) of all atoms were used in the calculation of the patterns. Parameters for the four water-hydrogen atoms in the dihydrate are

0020-1669/79/1318-3498$01.00/0